Colloidal particle foams: Templates for Au nanowire networks?

J. N. O'Shea, M. A. Phillips, M. D. R. Taylor, P. Moriarty, M. Brust, and V. R. Dhanak

Citation: Applied Physics Letters **81**, 5039 (2002); doi: 10.1063/1.1526924
View online: http://dx.doi.org/10.1063/1.1526924
View Table of Contents: http://scitation.aip.org/content/aip/journal/apl/81/26?ver=pdfcov
Published by the AIP Publishing

Colloidal particle foams: Templates for Au nanowire networks?

J. N. O'Shea, M. A. Phillips, M. D. R. Taylor, and P. Moriarty[a)]
School of Physics and Astronomy, University of Nottingham, Nottingham NG7 2RD, United Kingdom

M. Brust
Centre for Nanoscale Science, Department of Chemistry, University of Liverpool, Crown Street, Liverpool L69 7ZD, United Kingdom

V. R. Dhanak
Daresbury Laboratory, Warrington, Cheshire WA4 4AD, United Kingdom and Department of Physics, University of Liverpool, Liverpool L69 7ZE, United Kingdom

(Received 18 June 2002; accepted 14 October 2002)

Spin coating a dilute solution of thiol-passivated Au nanoparticles onto silicon produces nanostructured cellular networks. Photoemission measurements, coupled with atomic force microscopy imaging and a statistical crystallography analysis, show that although annealing in the 500–600 K range removes the thiol surfactants surrounding the nanoparticles, the cellular morphology of the nanocrystal foam is preserved following annealing. Thus, self-assembled nanocrystal arrays may be exploited as templates for (bare) Au nanostructures on Si. Although appreciable particle diffusion during annealing does not occur, significant sintering of Au nanocrystals within the cellular network branches is observed. © *2002 American Institute of Physics.* [DOI: 10.1063/1.1526924]

A fundamental goal of nanoscale science is the development of protocols to control the interactions, and thereby the ordering, of nanoparticles on solid substrates. The synthesis of long-range-ordered monolayers and films of colloidal nanocrystals has been a particular focus.[1–3] However, it is becoming increasingly clear that due to the rich physics and chemistry underlying the formation of nanoparticle arrays from colloidal suspensions, the likelihood of structures other than close-packed networks forming during solvent evaporation is very high. For example, pioneering work by Pileni *et al.*[4] and Ge and Brus[5] has shown that both hydrodynamic instabilities and spinodal decomposition can produce a diverse variety of nanocrystal patterns.

We have very recently demonstrated that nanostructured cellular networks or ''nanofoams'' may form when Au nanocrystals are spin coated onto a Si substrate.[6] A statistical crystallography[7] analysis illustrated that although the nanofoams shared features in common with prototypical cellular networks such as soap froths and biological tissues, they did not obey a fundamental law of statistical crystallography (namely Lewis' law)[7] and were far from statistical equilibrium. This is due to the imposition of a well defined correlation length during the spinodal decomposition process[6] that underlies the formation of the cellular network.

In this letter, we show that simply by annealing a nanocrystal cellular network at temperatures between 500 and 600 K, it is possible to remove the thiol surfactants surrounding the Au nanoparticles, yet preserve the cellular structure of the overlayer. Thus, the nanocrystal overlayer acts as a template for the formation of a network of Au nanowires which, as we also show, may be chemically bound to the underlying Si surface. A statistical crystallography analysis of tapping mode atomic force microscopy (TM-AFM) images shows that there are only minor changes in the network cell distribution before and after annealing.

A suspension of thiol [either dodecanethiol ($C_{12}H_{25}S$) or $C_5H_{11}S$]-passivated Au nanocrystals of 2 nm core diameter[8] in toluene was diluted appropriately in order to produce submonolayer coverages. 10 μL of the nanocrystal solution was spin coated onto either a native-oxide covered Si(111) sample or a hydrogen-passivated Si(111) surface prepared with well-established HF etching techniques.[9] TM-AFM was carried out using a Digital Instruments D3100 system. The photoemission measurements were taken on beamline 4.1 of the Synchrotron Radiation Source, Daresbury, U. K. using a Scienta SES200 hemispherical electron energy analyzer. All binding energies were referenced to the Fermi edge of the Ta sample holder. Due to the photon energy cutoff of the beamline (190 eV), C 1*s* spectra were acquired using a conventional unmonochromatized x-ray anode.

TM-AFM images of a cellular network taken before and after annealing at 500 K are shown in Figs. 1(a) and 1(b), respectively. Note that the nanocrystal overlayer is $\sim$3.6 $\pm$0.6 nm (i.e., the diameter of a pentanethiol-coated 2 nm Au particle) thick in Fig. 1(a). This increases to a value of 7.0 $\pm$3.0 nm in Fig. 1(b) due to the particle sintering discussed below. While the ''foamlike'' morphology of the nanocrystal overlayer both before and after annealing is clear from a cursory qualitative examination of the images shown in Fig. 1, a comprehensive quantitative structural analysis is possible using the techniques of statistical crystallography.[7]

The first step is to construct the Voronoi tessellation (equivalent to the Wigner–Seitz construction familiar from solid-state physics) associated with the centers of the network cells [inset of Fig. 1(c)]. We use a LABVIEW program to select the coordinates of the cell centers. These coordinates are passed to the QHULL utility[10] which returns the vertices of the polygons comprising the Voronoi tessellation. A second

a)Electronic mail: philip.moriarty@nottingham.ac.uk

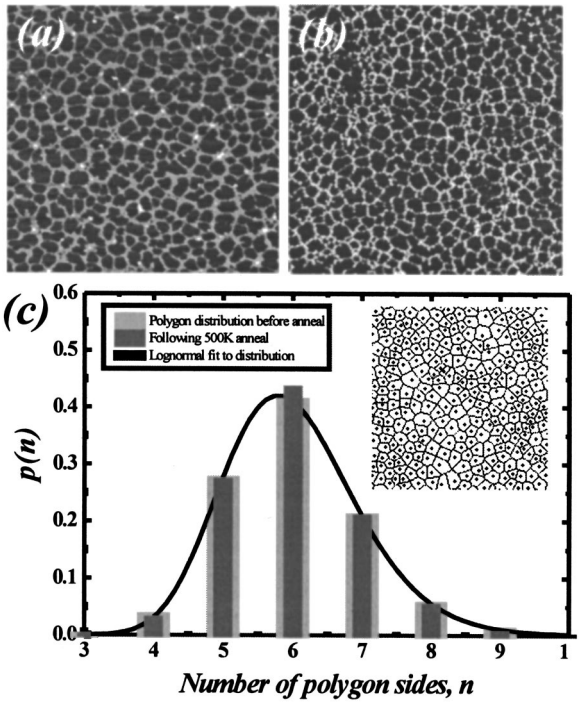

FIG. 1. A statistical crystallography analysis of nanostructured cellular networks formed by a submonolayer coverage of pentanethiol-terminated 2 nm Au nanoparticles on native oxide terminated Si(111). (a) and (b) TM-AFM images before and after 500 K anneal. (c) Histograms of polygon sidedness before and after annealing. (Inset: section of a typical Voronoi tessellation for a nanocrystal foam).

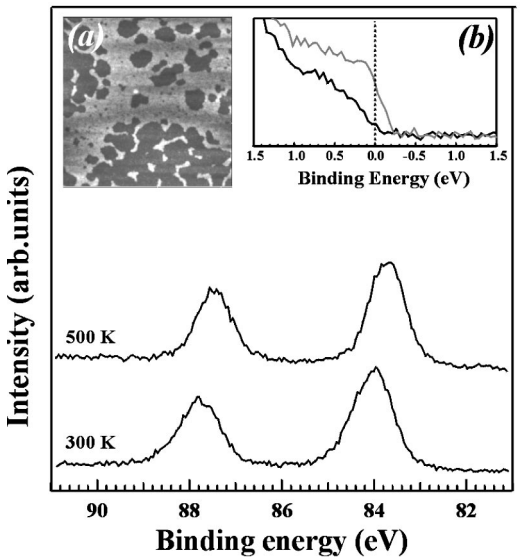

FIG. 2. Au $4f$ spectra ($h\nu$=190 eV) from C_5 thiol-passivated 2 nm Au nanocrystals on a native-oxide covered Si substrate before and after annealing at 500 K (normalized to unit height). Inset (a), a 1 μm square TM-AFM image, shows the morphology of this sample—note that the coverage is >1 monolayer. Inset (b) shows the shift in the Fermi edge position following annealing ($h\nu$=21.2 eV).

LABVIEW program then draws the tessellation and calculates the relevant statistical quantities.

Quantitative measures of the structural properties of the cellular network shown in Fig. 1(a) may be derived from an analysis of the distribution of polygon sidedness [$p(n)$, Fig. 1(c)]. First, the mean value of the number of polygon sides (both before and after annealing), $\langle n \rangle$, is 6.00, exactly that expected in the limit of an infinite network.[7] Our data set is, therefore, large enough to rule out statistical anomalies due to insufficient sampling. More importantly, the variance, $\mu_2 = \Sigma p(n)(n-\langle n \rangle)^2$, and entropy, $S = -\Sigma_n P_n \ln P_n$, of the side distribution from Fig. 1(c) are ~0.94 and 1.38, respectively, much lower than the values expected for a Poisson distribution of points (1.77 and 1.71, respectively).[7] This observation indicates that the positions of the cells are spatially correlated. The correlation arises from the presence of a specific spinodal wavelength during foam formation.[6]

Following annealing under ultrahigh vacuum (UHV) conditions at 500 K for 10 min (the temperature was monitored using an IR pyrometer), a number of TM-AFM images were acquired at macroscopically separated (mm's) regions of the sample surface. Although Fig. 1(b) was not acquired at the same region of the sample as Fig. 1(a), it is wholly representative of the morphology of the network following annealing—the properties of the foam vary little across the surface. Significantly, a tesselation analysis as described below yields very similar statistical quantities for the annealed network (μ_2=0.88, S=1.33). In addition, radially averaged Fourier transforms (not shown) yield identical intercellular correlation lengths of ~300 nm. Thus, even at relatively high temperatures, there appears to be negligible nanocrystal diffusion, supporting previous assertions[4,5] that colloidal nanocrystals have appreciable diffusion lengths on a substrate only in the presence of a solvent.

For a native-oxide-terminated Si substrate, annealing a coverage of Au nanocrystals at temperatures in the 500–600 K range induces relatively minor—though important—changes in the Au $4f$ spectra (Fig. 2). {Note that the spectra in Fig. 2 were from a different sample [see inset (a) of Fig. 2] to that shown in Fig. 1}. Following the anneal the Au $4f$ spectrum shifts by ~0.3 eV to lower binding energy (BE). We also observe a dramatic reduction (63%) in the integrated intensity of the C $1s$ peak, accompanied by a substantial increase in the Si $2p$ signal (not shown). The 63% reduction in the C $1s$ signal arises from the removal of the thiol groups encapsulating the Au nanocrystals (temperatures in excess of 1200 K are required to remove C from the near-surface region of Si samples). We also note that previous thermal desorption measurements of thiol monolayers on single-crystal Au surfaces have shown that chemisorbed thiolate desorbs between 500 and 620 K.[11]

The shift of the Au $4f$ peaks to ~0.3 eV lower BE following annealing is accompanied by a similar shift of the Fermi edge [see inset (b) of Fig. 2].[12] This shift is explicable by assuming that, prior to the removal of the thiol groups and on the time scale of the photoemission process, there is a slow rate of neutralization following the emission of a Au $4f$ photoelectron. This leads to Coulomb charging of the (low capacitance) nanoparticle, as discussed by Wertheim *et al.*[13] Annealing not only removes the electrically isolating thiol groups, but—due to sintering—also produces a continuous Au film for which Coulomb charging is not expected.

The loss of thiol groups on annealing is more strikingly highlighted when a H:Si(111) surface is used as a substrate. As shown in Fig. 3, the Au $4f$ line shape for 2 nm dodecanethiol-passivated clusters on HF-treated silicon broadens considerably following annealing at 500 K [Figs. 3(a) and 3(b)]. The Au–Si system is highly reactive: Au sil-

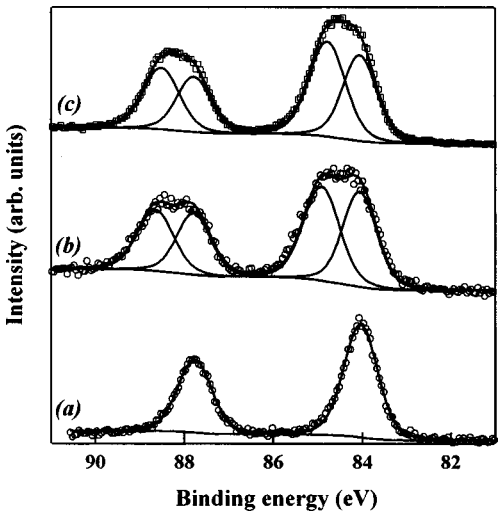

FIG. 3. (a) and (b) Au $4f$ spectra from dodecanethiol-passivated 2 nm Au nanocrystals on H:Si(111) before and after annealing at 500 K, respectively. (c) Au $4f$ spectrum from thick Au film deposited on a clean Si(111)-(7×7) surface. ($h\nu$=190 eV for all spectra.)

icide formation is observed for *room-temperature* deposition of Au on clean Si(111) surfaces.[14] A Au $4f$ spectrum for a thick gold film deposited on Si(111)-(7×7) under UHV conditions is shown in Fig. 3(c). Each of the spin–orbit split peaks can be fitted with a pair of asymmetric Voigt line shapes. The peak at a higher BE arises from Au silicide and is shifted by 0.75 eV with respect to the bulk Au peak.

Prior to annealing the nanocrystal/H:Si(111) sample, a single doublet is sufficient to fit the Au $4f$ core-level spectrum. Annealing at 600 K clearly induces the appearance of a second Au $4f$ component [Fig. 4(b)] with precisely the same BE shift as that measured for the Au silicide peak in Fig. 3(c). Thus, upon removing the surrounding thiol surfactants, the Au nanocrystals bind strongly to the underlying Si substrate. This provides a very simple method of fabricating

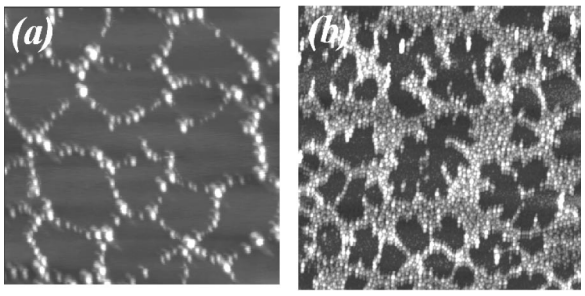

FIG. 4. (a) TM-AFM image highlighting internal structure of the branches of the network in Fig. 1(b) showing substantial nanoparticle sintering. (b) Breaks in the cellular network may be minimized by using higher submonolayer coverages of particles. Image size in both cases: 1 μm^2.

robust nanostructured Au cellular networks on silicon. Indeed, it should be possible to exploit the variety of nanocrystal patterns that form during solvent evaporation[4–6] to synthesize a diverse range of nanostructured films.

Although, as discussed above, the statistical properties of the cellular network do not change following a 600 K anneal, annealing produces significant sintering of the particles [Fig. 4(a)]. This leads to breaks in the Au network, severely compromising electrical conductivity. However, higher nanocrystal coverages [Fig. 4(b)] may be used to retain a percolating, though still cellular, Au network. [Note that the voids in Fig. 4(b) are reminiscent of those formed due to ''fingering instabilities'' in polymer films.[15] This point will be addressed in a future paper.]

Concluding, we have shown that it is possible to form Au cellular networks on silicon substrates using a self-assembled array of thiol-passivated nanoparticles as a template. In addition to having potential catalytic and sensor applications in its native state, the bare Au network may be functionalized to direct the adsorption of further species. The electrical and optical properties of these networks are currently under investigation.

Beamtime was provided by CLRC Daresbury Laboratory under Direct Access Award No. 37120. Financial support was from the U. K. EPSRC. One of the authors (M.B.) acknowledges EPSRC for an Advanced Research Fellowship (Ref. No. AF/100171). The authors thank George Miller for invaluable technical support.

[1] R. L. Whetten, J. T. Khoury, M. M. Alvarez, S. Murthy, I. Vezmar, Z. L. Wang, P. W. Stephens, C. L. Cleveland, W. D. Luedtke, and U. Landman, Adv. Mater. **8**, 428 (1996).
[2] P. J. Durston, J. Schmidt, R. E. Palmer, and J. P. Wilcoxon, Appl. Phys. Lett. **71**, 2940 (1997).
[3] R. P. Andres, T. Bein, M. Dorogi, S. Feng, J. I. Henderson, C. P. Kubiak, W. Mahoney, R. G. Osifchin, and R. Reifenberger, Science **272**, 1323 (1996).
[4] M. P. Pileni, J. Phys. Chem. B **105**, 3358 (2001).
[5] G. Ge and L. Brus, J. Phys. Chem. B **104**, 9573 (2000).
[6] P. Moriarty, M. D. R. Taylor, and M. Burst (unpublished).
[7] D. Weaire and N. Rivier, Contemp. Phys. **25**, 59 (1984).
[8] M. Brust, M. Walker, D. Bethell, D. J. Schiffrin, and R. Whyman, J. Chem. Soc. Chem. Commun. **7**, 801 (1994).
[9] P. Dumas, Y. J. Chabal, R. Gunther, A. T. Ibrahimi, and Y. Petroff, Prog. Surf. Sci. **48**, 313 (1995).
[10] C. B. Barber, D. P. Dobkin, and H. T. Huhdanpaa, *ACM Trans. on Mathematical Software*; http://www.geom.umn.edu/locate/qhull
[11] T. Shibue, T. Nakanishi, T. Matsuda, T. Asahi, and T. Osaka, Langmuir **18**, 1528 (2002).
[12] This shift is not due to static sample charging, as the Si $2p$ BE does not change.
[13] G. K. Wertheim, S. B. DiCenzo, and S. E. Youngquist, Phys. Rev. Lett. **51**, 2310 (1983).
[14] A. Kolmakov, S. Gunther, J. Kovac, M. Marsi, L. Casalis, K. Kaznacheev, and M. Kiskinova, Surf. Sci. **389**, 241 (1997).
[15] A. Sharma and G. Reiter, J. Colloid Interface Sci. **178**, 383 (1996).